

# An association between anisotropic plasma heating and instabilities in the solar wind

J. C. Kasper\* and B. A. Maruca  
*Harvard-Smithsonian Center for Astrophysics*

S. D. Bale

*Physics Department and Space Sciences Laboratory, University of California, Berkeley*

(Dated: September 3, 2018)

We present an analysis of the components of solar wind proton temperature perpendicular and parallel to the local magnetic field as a function of proximity to plasma instability thresholds. We find that  $T_{\perp p}$  is enhanced near the mirror instability threshold and  $T_{\parallel p}$  is enhanced near the firehose instability threshold. The increase in  $T_{\perp p}$  is consistent with cyclotron-resonant heating, but no similar explanation for hot plasma near the firehose limit is known. One possible explanation is that the firehose instability acts to convert bulk energy into thermal energy in the expanding solar wind, a result with significant implications for magnetized astrophysical plasma in general.

PACS numbers: 96.60.Vg, 96.50.Tf, 96.50.Ci, 95.30.Qd

*Introduction.*— Particle velocity distribution functions in the solar corona and solar wind are anisotropic, with separate temperatures  $T_{\perp}$  and  $T_{\parallel}$  relative to the magnetic field  $\mathbf{B}$  [1]. Characterizing the processes that create and limit temperature anisotropy is important for understanding heating and dynamical effects in solar physics [2] and in astrophysical plasmas in general [3]. Comprehensive *in situ* measurements of the solar wind by spacecraft are a unique way to investigate anisotropic plasmas and provide observational constraints for more exotic astrophysical objects such as accretion disks [4] and blazars [5]. The range of anisotropy seen in the solar wind is a result of competing phenomena: adiabatic expansion, heating through the anisotropic dissipation of waves, instabilities, and Coulomb collisions. Each of these factors has individually been the subject of intensive study; however, little work has been done on how the effects interact with and regulate each other. Our purpose here is to present the first observations of these interactions by looking at heating in the presence of instabilities. We begin with a review of anisotropy in the solar wind.

If solar wind protons expanded adiabatically, they would conserve the first and second CGL invariants so that  $T_{\perp p} \propto B$  and  $T_{\parallel p} \propto n_p^2/B^2$  [6], where  $p$  denotes protons and  $n_p$  is the number density. We would then expect  $R_p \equiv T_{\perp p}/T_{\parallel p} \propto B^3/n_p^2$ . The wind would then evolve along a particular trajectory in  $(\beta_{\parallel p}, R_p)$ -space, where  $\beta_{\parallel p} = n_p k_B T_{\parallel p} / (B^2/2\mu_0)$  is the ratio of the parallel pressure of protons to the magnetic pressure [7]. Observations have shown that while  $R_p$  decreases and  $\beta_{\parallel p}$  increases with distance from the Sun, the slope of the trajectory is inconsistent with adiabatic expansion. Specifically, an additional source of perpendicular heating must be introduced [7].

Evidence for perpendicular heating is common in regions such as the ionosphere, the solar wind, and the

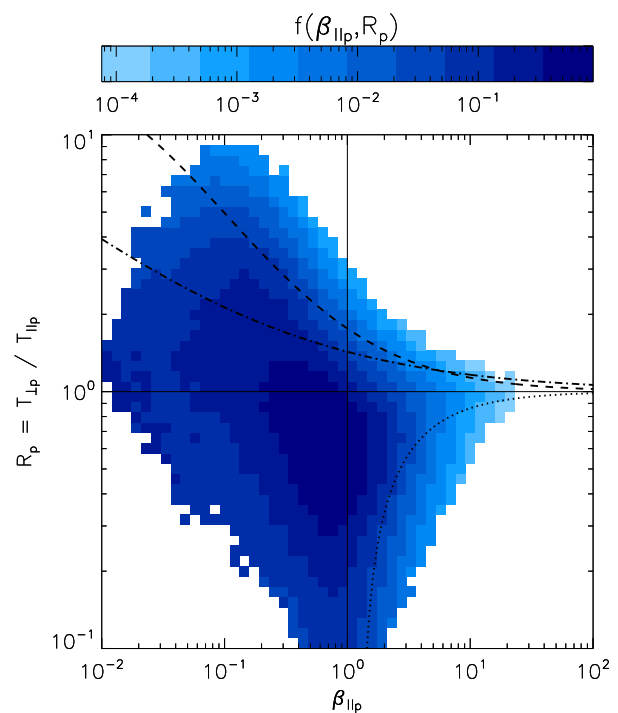


FIG. 1: The distribution function  $f$  of the solar wind in  $(\beta_{\parallel p}, R_p)$ -space at 1 AU. Lines are theoretical curves of constant growth rate for the firehose (dotted), mirror (dashed), and cyclotron (dot-dashed) instabilities. These instabilities bound a stable range of  $R_p$  as a function of  $\beta_{\parallel p}$ .

solar corona, where ions may develop  $R > 20$  [8]. One explanation is Alfvén-cyclotron dissipation, in which ions enter cyclotron resonance with compressive Alfvén waves on spatial scales near their gyro-radius and are preferentially energized perpendicular to  $\mathbf{B}$  [9, 10, 11]. Ion heating consistent with an Alfvén-cyclotron mechanism is also directly observed in interplanetary space [12].

Instabilities prevent expansion and heating from driving  $R_p$  arbitrarily far from unity. Fig. 1 is the probability

\*Electronic address: jkasper@cfa.harvard.edu

distribution  $f$  of the solar wind in  $(\beta_{\parallel p}, R_p)$ -space as measured by the *Wind* spacecraft at 1 AU. These observations are the focus of this letter and are described in more detail in the next section. Given the large anisotropies in the corona and the effects of adiabatic expansion, one would expect  $R_p$  to vary over orders of magnitude and be as small as  $10^{-3}$  [7, 13]. Instead we find  $0.1 \lesssim R_p \lesssim 5$  and constrained to a narrowing region near isotropy as  $\beta_{\parallel p}$  increases. This narrowing of  $f$  with  $\beta_{\parallel p}$  is attributed to instabilities, driven by  $R_p$ , that generate electromagnetic fluctuations, scatter particles in velocity space, and drive  $R_p$  toward unity. For  $R_p < 1$  and  $\beta_{\parallel p} \gtrsim 1$  the firehose instability can limit anisotropy [14], while for  $R_p > 1$ , the mirror and cyclotron instabilities are active [15, 16]. One way to quantify instabilities is to calculate the rate of growth of the unstable modes of the linear Vlasov equation. The three curves in Fig. 1 are contours of constant growth rate  $10^{-3}$  times the proton cyclotron frequency for each instability [15]. The sharp drop in  $f$  beyond these curves is interpreted as evidence of the instabilities. Comparing the shape of  $f$  with these curves, the mirror instability appears to be more important than the cyclotron instability at limiting  $R_p > 1$ , even though the amplitude of the cyclotron instability grows more quickly for  $\beta_{\parallel p} \leq 2$ . This diminished role for the cyclotron instability is supported by the recent discovery of enhanced magnetic fluctuations in plasma beyond the mirror and firehose threshold curves, but not the cyclotron threshold [13]. This surprising result, which highlights the potential pitfalls of linear theory, is possibly due to mirror fluctuations being more efficient at scattering particles in velocity space even if the growth rate is slower [15].

Having introduced the heating mechanisms and instabilities associated with temperature anisotropy in the solar wind, we now explore their interactions.

*Observations and analysis.*— Our study is motivated by an earlier work that examined the scalar temperature  $T_p = (2T_{\perp p} + T_{\parallel p})/3$  as a function of  $R_p$  and  $\beta_{\parallel p}$  and produced evidence suggesting plasma near the thresholds was hotter than expected [17]. This would be very interesting because the instabilities should not heat the plasma, only isotropize it. However, it was difficult to tell if the plasma was truly hotter near the instability thresholds, or if the result was due to the dependence of  $\beta_{\parallel p}$  on  $T_{\parallel p}$ . To better understand these associations, we use a more accurate set of temperature measurements and examine the components  $T_{\perp p}$  and  $T_{\parallel p}$  separately.

This study makes use of observations from two instruments on the *Wind* spacecraft: 92-second cadence ion velocity spectra from the Solar Wind Experiment Faraday Cup (FC) instruments [18] and 3-second measurements of  $\mathbf{B}$  from the Magnetic Field Investigation [19]. This merged dataset is publicly available and has been described in detail elsewhere [20]. In all of our earlier work, and to the best of our knowledge in all other determinations of anisotropy in the solar wind, higher time resolution  $\mathbf{B}$  values were averaged over each ion measurement.  $R_p$  was then determined by examining how  $T_p$

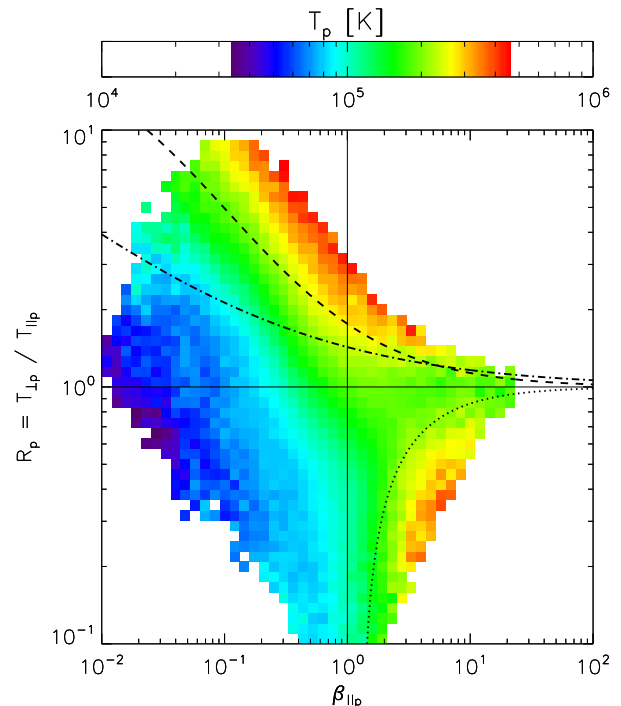


FIG. 2: Temperature  $T_p = (2T_{\perp p} + T_{\parallel p})/3$  as a function of  $R_p$  and  $\beta_{\parallel p}$ . Curves indicate theoretical thresholds due to instabilities. There is an overall trend of increasing  $T_p$  with  $\beta_{\parallel p}$ , which is expected since  $\beta_{\parallel p}$  is proportional to  $T_{\parallel p}$ , but there is also a clear association between the thresholds and hot plasma.

depends upon direction relative to the average  $\mathbf{B}$ . We realized that the strong magnetic fluctuations generated by unstable plasma [13] may create errors in  $R_p$  and rewrote our analysis to use the 3-second values of  $\mathbf{B}$ . This technique produces more accurate and often larger  $R_p$  when there are large fluctuations. While a detailed report on this method is in preparation, this letter contains our first result.

About 40% of the 4.1 million *Wind* ion spectra met our criteria for use in this study. We required the uncertainties in the derived temperatures to be less than 10%. We only used periods where *Wind* was far from the Earth's bow shock to avoid magnetospheric contamination. Finally, we only used observations where Coulomb relaxation was not an important factor. For each measurement, we calculated the Coulomb collisional age  $A_c$  defined as the number of small-angle Coulomb scatterings the plasma has experienced in the time it took to reach the spacecraft [12]. We then required  $A_c \leq 0.1$ .

We divided the selected observations into a  $50 \times 50$  grid of logarithmically-spaced bins in the  $(\beta_{\parallel p}, R_p)$ -plane. Within each bin, we calculated the number of observations  $N$  and the median value of  $T_p$ . For Fig. 1 we calculated  $f$  by dividing  $N$  by the width in  $\beta_{\parallel p}$  and  $R_p$  of each bin. Fig. 2 shows  $T_p$  for all  $(\beta_{\parallel p}, R_p)$ -bins with  $N \geq 50$ . Beyond a general tendency for  $T_p$  to grow with

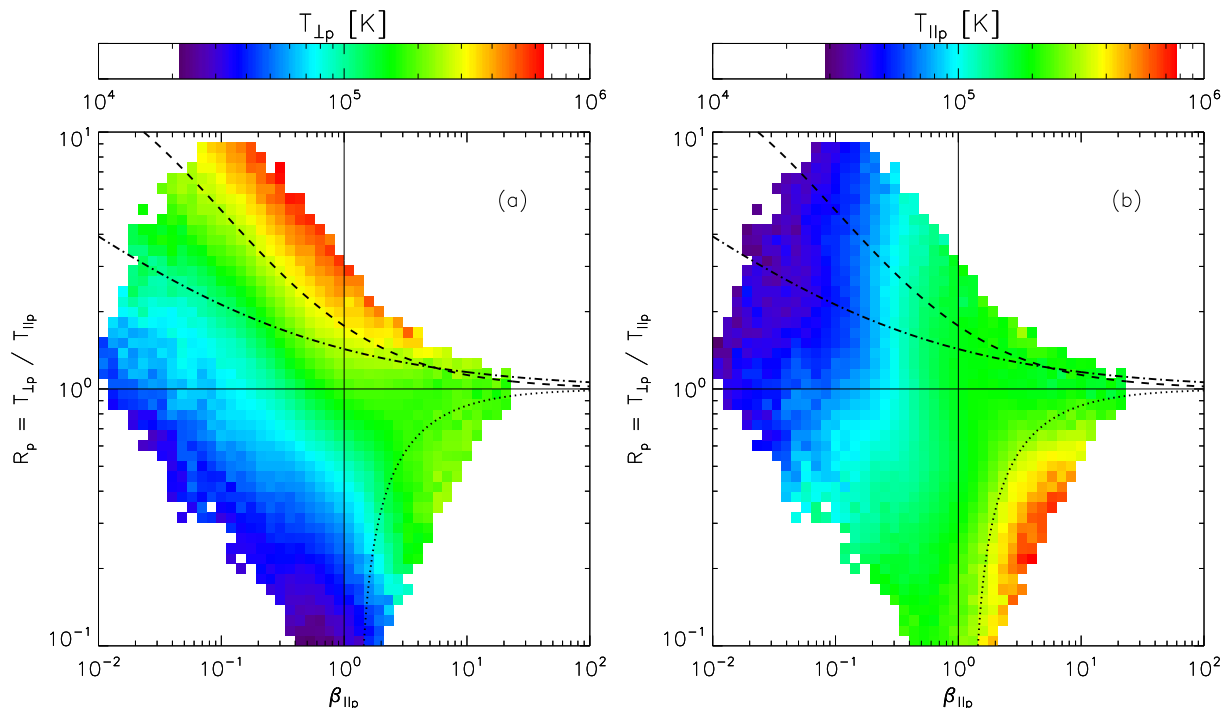


FIG. 3:  $T_{\perp p}$  (a) and  $T_{\parallel p}$  (b) over the  $(\beta_{\parallel p}, R_p)$ -plane. The increase in  $T_p$  is mainly in  $T_{\perp p}$  for plasma beyond the mirror threshold and in  $T_{\parallel p}$  for plasma beyond the firehose threshold.

$\beta_{\parallel p}$ , there are clearly two regions with enhanced  $T_p$ : one along the mirror instability threshold and the other along that of the firehose instability. Between these regions, even at high  $\beta_{\parallel p}$ , we see cooler plasma. For comparison,  $T_p \approx 1.8 \times 10^5$  K at  $(\beta_{\parallel p}, R_p) = (1, 1)$  but gets as high as  $T_p \approx 4.6 \times 10^5$  K, or nearly twice as hot, near the instability thresholds.

Fig. 2 conclusively establishes that there is a significant enhancement in  $T_p$  near the thresholds for anisotropy-driven instabilities, confirming the earlier suggestion of this effect [17]. There is a striking correlation between the region of increased  $T_p$  above the mirror and firehose thresholds and the region of enhanced magnetic fluctuations found by [13]. This result further confirms the role played by instabilities in limiting  $R_p$  in the solar wind and the idea that the mirror instability is more important than the cyclotron instability.

We have also calculated  $T_{\perp p}$  and  $T_{\parallel p}$  over the  $(\beta_{\parallel p}, R_p)$ -plane. The results, which are shown in Fig. 3, are dramatic: the heating near the mirror threshold is almost entirely  $\perp$  to  $\mathbf{B}$ , with  $T_{\perp p} \approx 6.4 \times 10^5$  K, while the heating near the firehose instability is  $\parallel$  to  $\mathbf{B}$ , with  $T_{\parallel p} \approx 7.7 \times 10^5$  K. Close inspection of Fig. 3 does show an increase, albeit smaller, in the other temperature component.

Consider the high temperature region near the mirror threshold. In Fig. 4 we plot the median values of  $T_{\perp p}$  and  $T_{\parallel p}$  as functions of  $R_p$  for all observations with  $3 \leq \beta_{\parallel p} \leq 30$ . Here we can clearly see that in addition to an increase in  $T_{\perp p}$  for  $R_p > 1$  there is also a slight increase in  $T_{\parallel p}$ . Since we do not expect the mirror instabil-

ity to heat the plasma directly, these results suggest the following interpretation. First, Alfvén waves enter cyclotron resonance with the protons, which increases  $T_{\perp p}$  and thus  $R_p$ . Eventually,  $R_p$  is sufficiently large that the mirror instability sets in and drives the plasma back toward isotropy. In doing so, some of the energy deposited into  $T_{\perp p}$  by anisotropic dissipation is transferred to  $T_{\parallel p}$ .

We now turn to the region near the firehose instability. Previous work suggests that the dominant mechanism producing  $R_p < 1$  is that CGL expansion cools  $T_{\perp p}$  more quickly than  $T_{\parallel p}$ , at least until the plasma reaches the firehose threshold [7]. Fig. 4 shows that  $T_{\perp p}$  is only slightly cooler for  $R_p < 1$  and  $3 \leq \beta_{\parallel p} \leq 30$ , while  $T_{\parallel p}$  is more than four times higher than typical wind, rising to 2 MK. This result suggests that a process is increasing  $T_{\parallel p}$ . One explanation is that there is an as-yet unknown dissipation mechanism in the solar wind that can raise  $T_{\parallel p}$ . There is little theoretical work on  $\parallel$  heating in the solar wind but other recent observational studies have reported cases of unusually large  $T_{\parallel p}$  [12]. A second possibility is that the heating arises directly as a result of the plasma being driven into the firehose instability by CGL expansion. Simulations of expanding wind have suggested that the firehose instability reduces  $T_{\parallel p}$  but also produces a high energy tail of particles  $\parallel$  to  $\mathbf{B}$  [21]. Perhaps this high energy tail subsequently relaxes and heats the plasma.

The energy for this speculative  $\parallel$  heating could come from slowing the solar wind down or by modifying the expansion of the magnetic field. The solar wind thermal energy is typically about 1/100 the kinetic energy. So for

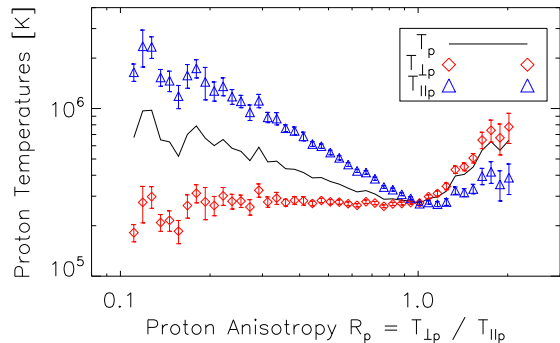


FIG. 4: Median scalar proton temperature  $T_p$  (black curve) and components  $T_{\perp p}$  (diamonds) and  $T_{\parallel p}$  (triangles) as a function of  $R_p$  for all observations with  $3 \leq \beta_{\parallel p} \leq 30$ . For  $T_{\perp p}$  and  $T_{\parallel p}$  uncertainty in the mean is indicated with error bars.

the largest  $T_{\parallel p}$  about 4% of the bulk energy of the wind would have to be converted into thermal energy.

*Conclusions.*— We have shown that protons with anisotropy beyond the mirror and firehose thresholds are 3 – 4 times hotter than those in typical solar wind. We examined  $T_{\perp p}$  and  $T_{\parallel p}$  and found that both components are hotter near each instability, but that most of the additional heating is in  $T_{\perp p}$  for  $R_p > 1$  and in  $T_{\parallel p}$  for  $R_p < 1$ . This result is interesting because instabilities are not understood to heat plasma themselves. The hot plasma is therefore either a signature of the interaction of instabilities with secondary processes or evidence that instabilities do more than merely redistribute thermal energy.

For  $R_p > 1$  we suggest that the high temperatures are due to a combination of an ion-cyclotron resonant heating process (such as dissipation of Alfvén waves) increasing  $T_{\perp p}$  and redistribution of thermal energy from  $T_{\perp p}$  into  $T_{\parallel p}$  by the mirror instability. A plasma undergoing slow

$\perp$  heating may achieve a state where the rate of injection of energy into  $T_{\perp p}$  is balanced by the redistribution of energy from  $T_{\perp p}$  into  $T_{\parallel p}$  by the mirror instability. Measurements of anisotropies alone therefore underestimate the level of heating from dissipation.

For  $R_p < 1$  the situation is less clear. Either there is an as-yet unidentified parallel heating mechanism at work in the solar wind, or the combination of CGL expansion and the firehose instability are capable of converting a small fraction of the bulk kinetic energy of the wind into thermal energy.

These results have implications beyond the solar wind. In any expanding plasma with  $\beta \gtrsim 1$ , the CGL-firehose association may be an effective mechanism for parallel heating and the generation of magnetic fluctuations. This result is directly applicable to heating and magnetic field generation in clusters of galaxies [22]. Our results also suggest a heating mechanism for contracting astrophysical plasmas. Consider, for example, accretion onto a compact object such as a black hole or a neutron star. There is a great deal of kinetic energy gained by the accreted matter as it falls into the gravitational potential well of the compact object. However, it is not understood how this kinetic energy is converted into thermal energy in the dynamical time of the infall. We have shown how expansion of the solar wind drives the plasma into the firehose instability and ultimately heats it. In the case of accretion, contraction of the plasma would instead drive  $R_p > 1$ , where the mirror instability might play an analogous role to the firehose instability in the solar wind, heating the accreting material while slowing the flow or shearing the magnetic field.

### Acknowledgments

JCK and BAM thank S. Cranmer, J. Raymond, and R. Narayan for discussions. Analysis of Wind observations is supported by NASA grant NNX08AW07G.

- 
- [1] A. Eviatar and M. Schulz, *Plan. Spa. Sci.* **18**, 321 (1970).
  - [2] J. A. Klimchuk, *Solar Phys.* **234**, 41 (2006).
  - [3] A. A. Schekochihin et al., *Astrophys. J. Supp.* **182**, 310 (2009), 0704.0044.
  - [4] P. Sharma, E. Quataert, G. W. Hammett, and J. M. Stone, *Astrophys. J.* **667**, 714 (2007).
  - [5] C. Röken and R. Schlickeiser, *Astronomy and Astrophysics* **503**, 309 (2009).
  - [6] G. F. Chew, M. L. Goldberger, and F. E. Low, *Royal Society of London Proceedings Series A* **236**, 112 (1956).
  - [7] L. Matteini et al., *Geophys. Res. Lett.* **34**, 20105 (2007).
  - [8] S. R. Cranmer, A. V. Panasyuk, and J. L. Kohl, *Astrophys. J.* **678**, 1480 (2008), 0802.0144.
  - [9] Y. Q. Hu and S. R. Habbal, *J. Geophys. Res.* **104**, 17045 (1999).
  - [10] S. R. Cranmer and A. A. van Ballegooijen, *Astrophys. J.* **594**, 573 (2003), arXiv:astro-ph/0305134.
  - [11] P. A. Isenberg and B. J. Vasquez, *Astrophys. J.* **668**, 546 (2007).
  - [12] J. C. Kasper, A. J. Lazarus, and S. P. Gary, *Physical Review Letters* **101**, 261103 (2008).
  - [13] S. D. Bale et al., *ArXiv e-prints* (2009), 0908.1274.
  - [14] J. C. Kasper, A. J. Lazarus, and S. P. Gary, *Geophys. Res. Lett.* **29**, 20 (2002).
  - [15] P. Hellinger et al., *Geophys. Res. Lett.* **33**, 9101 (2006).
  - [16] S. P. Gary and M. A. Lee, *J. Geophys. Res.* **99**, 11297 (1994).
  - [17] Y. Liu et al., *Journal of Geophysical Research (Space Physics)* **111**, 1102 (2006).
  - [18] K. W. Ogilvie et al., *Space Sci. Rev.* **71**, 55 (1995).
  - [19] R. P. Lepping et al., *Space Sci. Rev.* **71**, 207 (1995).
  - [20] J. C. Kasper et al., *J. Geophys. Res.* **111**, 3105 (2006).
  - [21] L. Matteini et al., *J. Geophys. Res.* **111**, 10101 (2006).
  - [22] A. A. Schekochihin et al., *Astrophys. J.* **629**, 139 (2005).